Internal Motions of the Rare Gas Atom in Dimethyl Ether−Krypton

Biagio Velino,[†] Sonia Melandri,[‡] and Walther Caminati*[,‡]

Dipartimento di Chimica Fisica e Inorganica dell'Università, Viale Risorgimento 4, I-40136 Bologna, Italy, and Dipartimento di Chimica "G. Ciamician" dell'Università, Via Selmi 2, I-40126 Bologna, Italy

Received: January 8, 2004; In Final Form: March 17, 2004

The free jet millimeter-wave absorption spectra of two isotopomers of the weakly bonded dimethyl ether−Kr complex have been assigned and measured. The Kr atom lies in the σ_v symmetry plane of dimethyl ether perpendicular to the COC plane, at a r_0-distance of 3.67 Å from its center of mass (*cm*). The line connecting the krypton atom to *cm* forms an r_0-angle of 70° with the O-*cm* line. The observed conformation is in agreement with the global minimum as found with a distributed polarizability model. Many rotational transitions are split into two component lines, due to the motion of Kr relative to dimethyl ether in the complex. The corresponding splitting has been used to determine the barrier to the internal motion. Information on the dissociation energy has been deduced from the centrifugal distortion effects.

Introduction

The nature of weak intermolecular interactions can be understood through the study of molecular adducts formed in a supersonic expansion. Various spectroscopic techniques have been used for this purpose,[1] but rotationally resolved spectroscopy has revealed itself to be particularly efficient and many adducts of organic molecules with a rare gas atom have been investigated in this way.[2] It has often been possible to observe even small vibrational splittings, which give precise information on the large-amplitude motions typical of this kind of adduct.

The most stable adducts between molecules and rare gas atoms are those involving cyclic aromatic molecules and the heavier rare gas atoms (Ar, Kr, and Xe). This is due, on one hand, to the presence of several interaction centers equidistant from the RG atom, and second to the higher polarizability of the heavier RG atoms with respect to the lighter ones. In these cases, the dissociation energy is estimated to be about 3−4 kJ/mol, and the rare gas atom appears to be located on one side of the ring and no inversion splitting has been observed.[3,4]

More recently, various less stable adducts between rare gases and open-chain molecules have been studied. From the inversion splittings, generally observed, it has been possible to derive information on the van der Waals vibrations. This is the case, for example, for acetaldheyde−Ar,[5−7] 1,1-difluoroethylene−Ne,[8] and difluoromethane−Ar.[9] Also the series of complexes of dimethyl ether with rare gases has been investigated. A wide splitting [807(1) MHz] was observed for dimethyl ether−Ne,[10] while a quite smaller splitting [0.9980(6) MHz] was measured for dimethyl ether−Ar.[11] From these splittings, the barriers to the rotation of the rare gas around dimethyl ether were estimated to be 0.19 and 0.69 kJ mol^{-1}, respectively. In the case of DME-Xe, no inversion splittings have been observed.[12]

Since Kr is intermediate between Ar and Xe, we decided to investigate the rotational spectrum of DME-Kr hoping to observe a tunneling splitting.

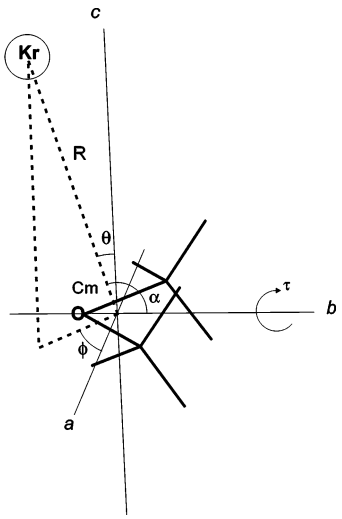

Figure 1. Sketch of DME-Kr. The parameters defining the position of the Kr atom, which will be used through the text, are also shown.

DME-Kr is schematically shown in Figure 1, together with the parameters defining the position of the Kr atom, which will be used through the text.

Experimental Section

DME and krypton were purchased from Aldrich and Rivoira, respectively.

The 60−78 GHz Stark and pulse-modulated free jet absorption millimeter-wave spectrometer used in this study has been described elsewhere.[13,14] The adduct was formed by mixing Kr and DME at room temperature and at partial pressures of ca. 800 and 10 mbar, respectively, and expanding the mixture to about 5×10^{-3} mbar through a pulsed nozzle (repetition rate 5 Hz) with a diameter of 0.35 mm, reaching an estimated "rotational" temperature of about 5−10 K. The accuracy of the frequency measurements was estimated to be 0.05 MHz. The signal-to-noise ratio was about 20/1 for the most intense absorption lines, when using a scan rate of 1 GHz/h and a time constant of 0.3 s.

* Corresponding author. Tel.: +39-051-2099480. Fax +39-051-2099456. E-mail: walther.caminati@unibo.it.
[†] Dipartimento di Chimica Fisica e Inorganica dell'Università.
[‡] Dipartimento di Chimica "G.Ciamician" dell'Università.

10.1021/jp0499068 CCC: $27.50
Published on Web 04/20/2004

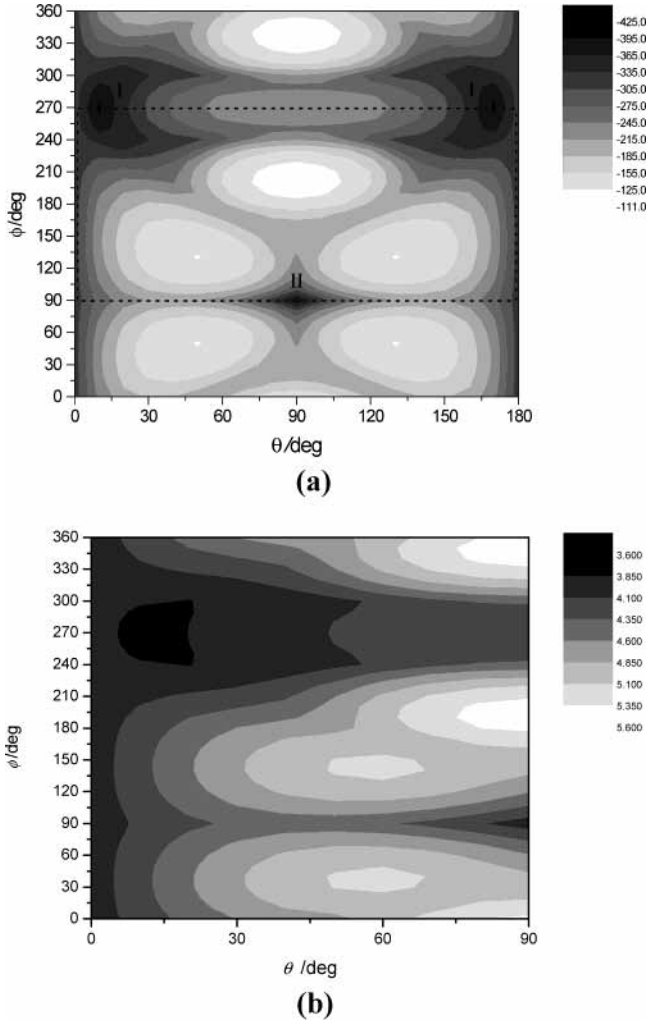

Figure 2. Results of the distributed polarizability model calculations. θ and φ are the spherical coordinates describing the position of Kr, as defined in the text. (a) $E(\theta,\phi)$, potential energy surface (cm^{-1}), in the full θ and ϕ ranges; (b) $R(\theta,\phi)$, surface describing the distance of Kr from the center of mass (Å); θ is considered only in the 0−90° range.

Calculation of the Potential Energy Surface with a Distributed Polarizability Model

The position of Kr in the complex can be described with spherical coordinates R, θ, and ϕ, shown in Figure 1. R is the distance of the Kr atom from the center of mass of the monomer, θ is the angle that the R vector makes with the c inertial axis of DME, and ϕ is the angle between the projection of R in the ab plane and the a inertial axis of DME.

The potential energy and R have been evaluated as functions of θ and ϕ by using a distributed polarizability model (DPM).[15] The calculations have been performed with the computer program RGDMIN.[16] In the calculation the geometry of the monomer was held fixed to its r_s values,[17] while R was optimized in the ranges $\theta = 0-180°$ and $\phi = 0-360°$ with steps of $\Delta\theta = \Delta\phi = 10°$. Three minima were found, as shown in the two-dimensional surface drawn in Figure 2; two of them correspond to equivalent positions above and below the COC plane of DME while the third one, slightly higher in energy, sees the Kr atom lying in the COC plane. Those points were subsequently characterized by unconstrained DPM and the derived geometries and energies, reported in Table 1, were used as an initial guess for the assignment of the rotational spectrum.

TABLE 1: Relative Energies, Spherical Coordinates, and Rotational Constants of the Two Configurations of DME-Kr[a]

	conf. I	conf. II	exptl.[b]
$\Delta E_{DPM}/cm^{-1}$	0	11	
R/Å	3.765	3.977	3.674[c]
θ/deg	9.83[d]	90.	20.2[c]
ϕ/deg	270.	90.	270[c]
A/MHz	8982.2	10111.1	9067.9
B/MHz	1169.5	1046.0	1221.0
C/MHz	1076.8	959.6	1116.3

[a] The DPM calculated rotational constants are compared to the experimental values. [b] ^{84}Kr isotopomer. [c] r_0 values, see ahead. [d] $\theta = 170.17$ corresponds to an equivalent point.

TABLE 2: Experimental Transition Frequencies (MHz) of DME-Kr

	^{84}Kr		^{86}Kr	
$J'(K_a',K_c') \leftarrow J''(K_a'',K_c'')$	$0^+ \leftarrow 0^-$	$0^- \leftarrow 0^+$	$0^+ \leftarrow 0^-$	$0^- \leftarrow 0^+$
4(4)−3(3)[a]	64636.90	64636.58	64627.28	64626.93
5(4)−4(3)[a]	66966.75	66966.41	66939.36	66939.04
5(5)−5(4)[a]	71091.14[b]			
6(4)−5(3)[a]	69294.73	69294.46	69249.70	69249.43
6(5)−6(4)[a]	71082.24	71082.11		
7(4)−6(3)[a]	71620.75	71620.34		
7(5)−7(4)[a]	71071.44	71071.29		
8(4,5)−7(3,5)	73944.26[b]		73864.00[b]	
8(4,4)−7(3,4)	73943.00[b]		73862.62[b]	
8(5)−8(4)[a]	71058.32[b]			
9(3,7)−8(2,7)	60559.41	60559.07	60441.60	60441.25
9(3,6)−8(2,6)	60349.05	60348.71	60237.63	60237.33
9(4,6)−8(3,6)	76265.18[b]		76167.55	76167.24
9(4,5)−8(3,5)	76262.36[b]		76164.72	76164.57
9(5)−9(4)[a]	71043.15[b]			
10(3,8)−9(2,8)	62923.16	62922.82	62786.54	62786.21
10(3,7)−9(2,7)	62595.56	62595.20	62468.62	62468.48
10(5)−10(4)[a]	71025.36[b]			
11(3,9)−10(2,9)	65298.31	65297.95	65142.56	65142.27
11(3,8)−10(2,8)	64812.17	64811.80	64670.95	64670.68
11(5)−11(4)[a]	71004.86[b]			
12(3,10)−11(2,10)	67687.23	67686.80		
12(3,9)−11(2,9)	66993.92	66993.58		
12(5)−12(4)[a]	70981.29[b]			
13(3,11)−12(2,11)	70092.37	70092.02		
13(3,10)−12(2,10)	69136.24	69135.93		
14(2,13)−13(1,13)	61106.90[b]			
15(2,14)−14(1,14)	64166.35[b]			
16(2,15)−15(1,15)	67276.80[b]			
17(2,16)−16(1,16)	70437.90[b]			

[a] Transitions doubly overlapped due to the near prolate degeneracy of the involved levels; only K_a is given. [b] Transitions not resolved for the doubling due to the tunneling motion.

Rotational Spectra

The first search for the spectrum of the complex was based on the rotational constants of the global minimum described above (first column of Table 1). In going from the molecule to the adduct, the directions of the principal axes of inertia with respect to the ring skeleton change, so that the μ_b-type spectrum of DME is converted into a predominant μ_c-type spectrum in the adduct. Also a weak μ_a-dipole moment component is expected, which is useful for Stark modulation. The rotational spectrum of the ^{84}Kr species (∼57% of natural abundance) was investigated first. Thirty μ_c-type transitions have been measured; most of them were R-type lines, with J ranging from 4 to 17, although the Q-branch with $K_a = 5 \leftarrow 4$ was measured too. Many transitions were split into two component lines separated by 0.3−0.4 MHz, showing unequivocally that a tunneling motion which inverts the μ_c-dipole moment component takes place through the COC plane of DME. The spectrum of the ^{86}Kr species (∼17% of natural abundance) was then measured also, showing the same features of the^{84}Kr spectrum. The measured transitions, listed in Table 2, could be fit with a

TABLE 3: Spectroscopic Constants of Normal and ^{86}Kr Isotopic Species of DME-Kr

	^{84}Kr		^{86}Kr	
	0^+	0^-	0^+	0^-
A (MHz)	9067.92(3)[a]	9067.91(3)	9067.8(1)	9067.8(1)
B (MHz)	1221.01(1)	1221.01(1)	1211.36(5)	1211.35(5)
C (MHz)	1116.28(1)	1116.28(1)	1108.19(5)	1108.19(5)
$\Delta E_{0^+-0^-}$ (MHz)	0.26(5)		0.26(8)	
D_J (kHz)	4.48(1)		4.37(3)	
$_K$ (kHz)	74.7(1)		74.(1)	
D_K (kHz)	54.(1)		55.(5)	
d_1 (kHz)	−0.36(1)		−0.36[b]	
d_2 (kHz)	−0.082(2)		−0.082[b]	
N[c]	46		24	
σ[d] (MHz)	0.06		0.06	

[a] Errors in parentheses are in units of the last digit. [b] Fixed to the normal species value. [c] Number of transitions in the fit. [d] Standard deviation of the fit.

Pickett-type coupled Hamiltonian,[18,19] here given in its simpler form:

$$H = H_R(0^+) + H_R(0^-) + H_{CD} + \Delta E \quad (1)$$

where $H_R(0^+)$ and $H_R(0^-)$ represent the rigid rotational parts of the Hamiltonian for the 0^+ and 0^- states, respectively. The centrifugal distortion contributions (S-reduction and I^r-representation[20]) are represented by H_{CD}, and were assumed to be the same in both states. The determined spectroscopic constants are presented in Table 3.

Location of the Kr Atom in the Complex

Planar moments of inertia are defined as $P_{aa} = \sum_i m_i a_i^2$, with $i = 1$, N (N = number of atoms), etc., and are obtained directly from the rotational constants through: $P_{aa} = (h/16\pi^2)\,[-1/A + 1/B + 1/C]$, etc. They characterize, approximately, the extension of the mass distribution along the respective axis being very useful to rapidly locate the position of a rare gas in a complex such as DME-Kr.

The value of the planar moment of inertia P_{bb} of the complex (47.283 uÅ^2) is very similar to that of P_{aa} of isolated DME (47.047 uÅ^2). Although caution is needed in getting structural information from these data, due to the Coriolis effects of the large-amplitude motions of RG),[21] we believe that the similar values of the two planar moments of inertia strongly support the hypothesis that the Kr atom lies in the σ_v plane of symmetry of DME perpendicular to the COC plane.

Three different sets (r_0, r_s, and r_{DPM}) of the van der Waals structural parameters of the complex are shown in Table 4. R is the distance between the center of mass of the monomer and the Kr atom, and α is the angle that the line connecting the krypton atom to the center of mass of DME (Kr-*cm*) forms with the bisector of the COC angle (see Figure 2).

The r_0 geometry has been obtained fitting R_{cm} and α to the available rotational constants. The geometry of DME has been fixed to that of the isolated molecule,[17] and Kr has been assumed to lie in the σ_v plane of symmetry of DME.

The r_s coordinates[22] of the krypton atom (bottom of Table 4), can be obtained in the principal axes system of DME by a hypothetical substitution of an atom of zero mass with a krypton atom in going from DME to DME-Kr or in the principal axes of DME-^{84}Kr when substituting ^{84}Kr with ^{86}Kr. Owing to the Coriolis effects of van der Waals vibrations they are indicative values only. The r_s values are indeed rather different with respect to the r_0 parameters (see Table 4).

TABLE 4: van der Waals Structural Parameters

(a) van der Waals Parameters (Å and °)

	r_0[a]	r_s	R_{DPM}[b]
R_{cm}	3.674(3)[c]	3.673	3.765
a	110.2(2)	117.0	99.8

(b) Kr r_s coordinates (Å)

	PAS$_{DME}$[d]		PAS$_{DME\cdots Kr}$[e]	
	exptl.	calc.[f]	exptl.	calc.[f]
$\|x\|$	1.666(4)[g]	1.268	0.00	0.013
$\|y\|$	0.259(4)	0.0[h]	0.00	0.0[h]
$\|z\|$	3.284(3)	3.448	1.295(1)	1.273

[a] From the fit of rotational constants. [b] See text. [c] Error (in parentheses) is expressed in units of last digit. [d] Hypothetical isotopic substitution of an atom of zero mass with a ^{84}Kr. Coordinates in the principal axes system of DME [e] Isotopic substitution ^{84}Kr → ^{86}Kr. Coordinates in the principal axes system of DME-^{84}Kr. [f] Calculated with the r_0 parameters above. [g] Errors in parentheses are just fitting errors, with little physical meaning; see text. [h] By symmetry.

TABLE 5: Potential Energy Parameters for the RG Motions in DME-RG[a]

	Kr[b]	Ne[c]	Ar[d]	Xe[e]
k_S (Nm^{-1})	2.6	1.0	2.3	3.0
ν_s (cm^{-1})	38	36	42	39
E_B (kJ mol^{-1})	2.9	1.0	2.5	3.7
V_{inv} (cm^{-1})	1.33	0.19	0.69	

[a] See text for definitions. [b] This work. [c] From ref 10. [d] From ref 11. [e] From ref 12.

The r_{DPM} geometry (also in Table 3) has been obtained as described in the polarizability model section.

van der Waals Vibrations and Dissociation Energy

(a) Kr Stretching and Dissociation Energy. First we assumed the Kr stretching motion to be isolated from the other motions, and estimated the stretching force constant (k_s) by approximating the complex as a molecule made up of two rigid parts. Millen,[23] for complexes with several symmetry elements and Read et al.,[24] for asymmetric top complexes in which the stretching coordinate is near-parallel to the inertial a-axis, obtained equations of the following type:

$$k_s = 16\pi^4(\mu R_{cm})^2[4B^4 + 4C^4 - (B-C)^2(B+C)^2]/(hD_J) \quad (2)$$

where B, C, and D_J are rotational and centrifugal distortion constants of the adduct, μ is the pseudo-diatomic reduced mass, and R_{cm} is the distance between the centers of mass of the monomers (3.673 Å for DME-Kr). We obtained $k_s = 2.56$ Nm^{-1}, corresponding to a harmonic stretching fundamental of wavenumber $\nu_k = 38$ cm^{-1}.

By assuming a Lennard-Jones type potential, the dissociation energy has been estimated by applying the approximate formula[25]

$$E_B = 1/72\; k_s\, R_e^2 \quad (3)$$

The value $E_B = 2.9$ kJ/mol has been calculated, intermediate between the corresponding values of DME-Ar and DME-Xe (see Table 5).

(b) Tunneling Motion of the Kr Atom with Respect to DME. The vibrational splitting of Table 3, $\Delta E_{0^+-0^-} = 0.26$-(5) MHz), has been used to determine the potential energy barrier between the two equivalent minima I of Figure 2, by using Meyer's one-dimensional flexible model.[26] This model allows us to calculate the vibrational spacings, but needs a description of the pathway and a potential energy function. With

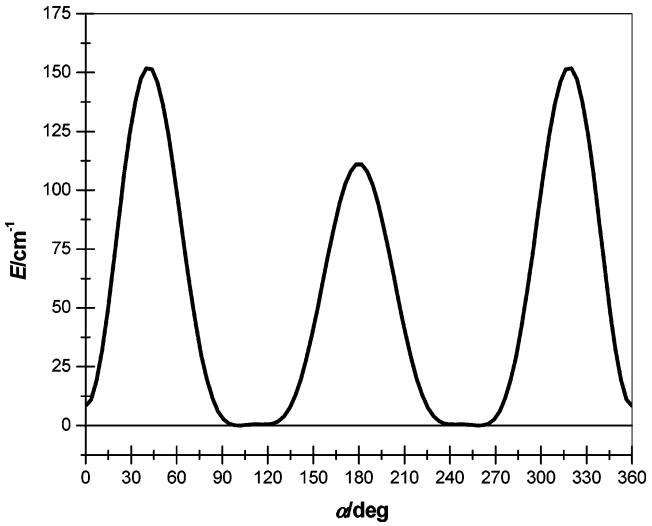

Figure 3. Energy profile of the tunneling motion of Kr, described by the α-coordinate in the symmetry plane of DME-Kr perpendicular to the COC plane.

reference to Figure 2, which is a planisphere, we can individuate the tunneling pathway along the broken line, which includes the three energy minima (two of them equivalent to each other). The vertical segments of the broken line, at $\theta = 0°$ and $\theta = 180°$, correspond to single points, the poles of the surface in a spherical representation. This pathway takes place in the symmetry plane of DME perpendicular to the COC plane, and it is described by coordinate α of Figure 1. Apparently the spherical coordinate θ could have been used to describe this cyclic motion, but, since it is defined only in the range 0°−180°, it is not appropriate for this purpose. The potential energy maxima and minima found along the pathway can be reproduced with the following function:

$$V(\alpha)/\mathrm{cm}^{-1} = V'(\cos\alpha - \cos\alpha_0)^2\,(1 - 0.95\cos 3\alpha)\,(1 + 0.17\cos\alpha) \quad (4)$$

where the factor $(\cos\alpha - \cos\alpha_0)^2$ fixes the position of the two equivalent minima and the remaining part the relative values of the other stationary points.

Correspondingly, the relaxations of R as a function of α can be represented, according to Figure 2(b) as

$$R(\alpha)/\text{Å} = R_0 + \Delta R(\cos\alpha - \cos\alpha_0)^2\,(1 - 0.95\cos 3\alpha)\,(1 + 0.17\cos\alpha) \quad (5)$$

where the values R_0 and $\Delta R = 3.67$ and 0.40 Å have been used, respectively.

Equations (4) and (5) have been used, within the flexible model mentioned above, to calculate the $\Delta E_{0^+-0^-}$ vibrational spacing. In the calculations the 2π cyclic range was resolved into 45 mesh points.[26]

To reproduce the experimental splitting we had to change the variable (scaling) parameter V' from 130 (corresponding to the DPM calculations) to 102 cm^{-1}. The profile of $V(\alpha)$ is given in Figure 3. One can see that the tunneling between the two equivalent minima, at $\alpha \cong \pm 105°$, can take place through two planar configurations with the Kr atom in the side of the oxygen atom or of the two methyl groups. The former path appears easier, either because the barrier to inversion is lower ($V_{inv} \sim 112\ \mathrm{cm}^{-1}$) or the angular distance shorter (≈150°). In addition the second path requires the crossing of two (higher) barriers, at $\alpha \cong \pm 40°$.

The comparison with the inversion barriers for the homologous complexes DME-Ar and DME-Ne is not straightforward, because in those cases the preferential pathways were along the τ coordinate of Figure 1. The tunneling barrier is higher, however, in the Kr case.

Conclusions

The features of the millimeter-wave free jet absorption rotational spectrum of DME-Kr have been useful to model the potential energy surface of the motions of the Kr atom in the complex. Supplementary information has been obtained from distributed polarizability model calculations. This model seems to indicate that the pathway of the tunneling internal rotation of Kr takes place along the symmetry plane of the complex. The pathway appears to be different with respect to those found for the complexes of DME with the lighter noble gas atoms Ne and Ar, where the tunneling motion takes place along the τ coordinate. The values of the inversion barriers V_{inv} increase, as expected, in going from Ne to Kr, as shown in Table 5.

The DPM potential energy surface for the tunneling motion had to be reduced by 30% in order to account for the observed inversion splitting.

Acknowledgment. We thank Mr. A. Millemaggi for technical help, and the Ministero dell' Universita' e della Ricerca Scientifica e Tecnologica, and the C.N.R. for financial support

References and Notes

(1) *Atomic and Molecular Beam Methods*; Scoles, G., Ed.; Oxford University Press: New York, 1988.
(2) Novick, S. E. Bibliography of Rotational Spectra of Weakly Bound Complexes, 2003, available at http://www.wesleyan.edu/chem/faculty/novick/vdw.html.
(3) Kukolich, S. G.; Shea, J. A. *J. Chem. Phys*. **1982**, *77*, 5242.
(4) Brupbacher, Th.; Makarewicz, J.; Bauder, A. *J. Chem. Phys*. **1994**, *101*, 9736−9746.
(5) Ioannu, I. I.; Kuczkowski, R. L. *J. Mol. Spectrosc*. **1994**, *166*, 354−364.
(6) Ioannu, I. I.; Kuczkowski, R. L.; Hougen, J. T. *J. Mol. Spectrosc*. **1995**, *171*, 265−286.
(7) Melandri, S.; Dell'Erba, A.; Bavero, P. G.; Caminati, W. *J. Mol. Spectrosc*. **2003**, *222*, 121−128.
(8) Dell'Erba, A.; Melandri, S.; Millemaggi, A.; Caminati, W.; Favero, P. G. *J. Chem. Phys*. **2000**, *112*, 2204−2209.
(9) Lopez, J. C.; Favero, P. G.; Dell'Erba, A.; Caminati, W. *Chem. Phys. Lett*. **2000**, *316*, 81−87.
(10) Maris, A.; Caminati, W. *J. Chem. Phys*. **2003**, *118*, 1649−1652.
(11) Ottaviani, P.; Maris, A.; Caminati, W.; Tatamitani, Y.; Suzuki, Y.; Ogata, T.; Alonso, J. L. *Chem. Phys. Lett*. **2002**, *361*, 341−348.
(12) Favero, L. B.; Velino, B.; Millemaggi, A.; Caminati, W. *ChemPhysChem* **2003**, *4*, 881−884.
(13) Melandri, S.; Caminati, W.; Favero, L. B.; Millemaggi, A.; Favero, P. G. *J. Mol. Struct*. **1995**, *352/353*, 253−258.
(14) Melandri, S.; Maccaferri, G.; Maris, A.; Millemaggi, A.; Caminati, W.; Favero, P. G. *Chem. Phys. Lett*. **1996**, *261*, 267−271.
(15) (a) Kisiel, Z. *J. Phys. Chem*. **1991**, *95*, 7605. (b) Kisiel, Z.; Fowler, P. W.; Legon, A. C. *J. Chem. Phys*. **1991**, *95*, 2283.
(16) Kisiel, Z. *PROSPE−Programs for Rotational Spectroscopy*; available at http://info.ifpan.edu.pl/~kisiel/prospe.htm.
(17) Lovas, F. J.; Lutz, K.; Dreizler, H. *J. Phys. Chem. Ref. Data* **1979**, *8*, 1051.
(18) Pickett, H. M. *J. Chem. Phys*. **1972**, *56*, 1715−1723.
(19) Pickett, H. M. *J. Mol. Spectrosc*. **1991**, *148*, 371−377.
(20) Watson, J. K. G. In *Vibrational Spectra and Structure*; Durig, J. R., Ed.; Elsevier: New York/Amsterdam, 1977; Vol. 6, pp 1−89.
(21) Caminati, W.; Favero, P. G.; Melandri S.; Meyer, R. *Chem. Phys. Lett*. **1997**, 268, 393−400.
(22) Kraitchman, J. *Am. J. Phys*. **1953**, *21*, 17−25.
(23) Millen, D. J. *Can. J. Chem*. **1985**, *63*, 1477−1479.
(24) Read, W. G.; Campbell, E. J.; Henderson, G. *J. Chem. Phys*. **1983**, *78*, 3501−3508.
(25) Bettens, R. P. A.; Spycher, R. M.; Bauder, A. *Mol. Phys*. **1995**, *86*, 487−511.
(26) Meyer, R. *J. Mol. Spectrosc*. **1979**, *76*, 266−300.